ACS OMEGA

http://pubs.acs.org/journal/acsodf

Article

# Polymer Brushes on GaAs and GaAs/AlGaAs Nanoheterostructures: A Promising Platform for Attractive Detection of *Legionella pneumophila*

Juliana Chawich, Walid M. Hassen, Amanpreet Singh, Daniela T. Marquez, Maria C. DeRosa, and Jan J. Dubowski*

Cite This: *ACS Omega* 2022, 7, 33349−33357

Read Online

ACCESS | Metrics & More | Article Recommendations | Supporting Information

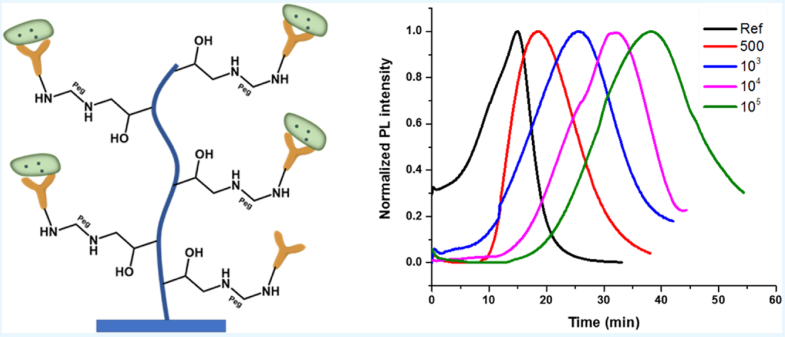


**ABSTRACT:** This work reports on the potential of polymer brushes (PBs) grown on GaAs substrates (PB-GaAs) as a promising platform for the detection of *Legionella pneumophila (Lp)*. Three functionalization approaches of the GaAs surface were used, and their compatibility with antibodies against *Lp* was evaluated using Fourier transform infrared spectroscopy and fluorescence microscopy. The incorporation of PBs on GaAs has allowed a significant improvement of the antibody immobilization by increased surface coverage. Bacterial capture experiments demonstrated the promising potential for enhanced immobilization of *Lp* in comparison with the conventional alkanethiol self-assembled monolayer-based biosensing architectures. Consistent with an eightfold improved capture of bacteria on the surface of a PB-functionalized GaAs/AlGaAs digital photocorrosion biosensor, we report the attractive detection of *Lp* at 500 CFU/mL.



## 1. INTRODUCTION

*Legionella pneumophila (Lp)* is a pathogenic waterborne bacterium that has been recognized as a source of infection through inhalation of aerosolised contaminated water,[1] leading to outbreaks of Legionellosis and Pontiac fever,[2,3] resulting in morbidity and mortality. The detection and monitoring of *Lp* in water sources and man-made artificial water systems have thus become a major public health concern worldwide.[4−6]

Culture-based methods commonly used for the detection of *Lp* are mainly constrained by the multi-day delay of incubation for visible detection of bacterial colonies[7] and the inability of some culture media to support the growth of viable bacteria.[8] Other conventional techniques for the identification and detection of *Lp*, such as polymerase chain reaction[9] and matrix-assisted laser desorption ionization time-of-flight spectroscopy,[10] generally provide fast and accurate results, but often require the use of sophisticated equipment and highly qualified personnel.

In the past few decades, biosensor technology has emerged as an alternative platform for providing rapid, sensitive, and potentially cost-attractive detection of pathogenic *Lp*,[11] with possibility of automation and regeneration. Numerous biosensing methods have been proposed to detect *Lp*, including surface plasmon resonance[12] and electrochemical impedance spectroscopy.[13] Despite the large market potential and the significant progress achieved, the aforementioned biosensors suffer from drawbacks, such as the high cost of materials, the difficulty to automate and reuse the biosensor, and the need for relatively bulky equipment.

Recently, GaAs semiconductors have gained increasing interest due to their compatibility with acoustic[14] and photoluminescence (PL)[15,16] biosensing techniques, demon-

Received: June 24, 2022
Accepted: August 23, 2022
Published: September 6, 2022





https://doi.org/10.1021/acsomega.2c03959
*ACS Omega* 2022, 7, 33349−33357

strating a remarkable potential for rapid and sensitive detection of bacteria. A PL-monitored digital photocorrosion (DIP) biosensor using GaAs/AlGaAs nanoheterostructures has provided a compelling platform for the detection of *Escherichia coli* K12 at $10^3$ CFU/ml[17,18] and *Lp* ssp1 at $2 \times 10^2$ CFU/mL.[19,20]

The selection of the biorecognition elements or ligands is a crucial primary step to achieve sensitive and selective detection of *Lp*. Several ligands have been reported in the literature for capturing *Lp*, including aptamers,[21] antibodies,[16] nucleic acids,[22] and peptides.[20] Among these, antibodies remain most commonly used due to their exquisite target specificity and affinity and their wide variety of immobilization strategies.[23] Undeniably, the efficiency of the immobilization method is extremely critical for the optimization of specific interactions between the antibody and the medium to be analyzed. It can affect the orientation, the density, and the accessibility of the ligands.[24] Oriented immobilization of antibodies has shown to effectively enhance their antigen-binding activity, and avoid their denaturation or the blocking of their active site.[25] Particularly, functionalization with protein A has proven to have a significant positive impact on biosensing performance, as it ensures that IgG antibodies are anchored on the substrate surface through their Fc portion and that binding sites located on the Fab region remain free and easily accessible for antigen binding, thus increasing the sensitivity of the detection.[26]

The detection of *Lp* has been also addressed using a variety of surface functionalization chemistries. Recently, the limited success of self-assembled monolayers (SAMs) in sensitive bacteria detection has generated growing interest in exploring alternative architectures, such as those based on polymer brushes (PBs). The attractive three-dimensional character of PBs, combined with the possibility of modifying their end functional groups, has made their use an innovative biosensing strategy, allowing to minimize non-specific interactions, thus leading to optimized biosensing performances and significantly improved limits of detection.[27−29] The growing interest in incorporating PBs on semiconductors such as silicon, silicon carbide, and graphene substrates[30−32] has been a driving force to the development of optimized incorporation strategies to facilitate biosensor manufacturing and enhance their performance.[33−35]

In an attempt to address the detection of bacteria using a GaAs-based biosensor, the incorporation of PBs on GaAs has been previously reported, and different methodologies were investigated to prepare and tune PBs on the GaAs surface.[36] The potential of PB-GaAs as a useful platform for antibody grafting was demonstrated by the binding of antibodies against *E. coli* and *Lp* and the superior control of nonspecific interactions. As a follow up, the potential of PBs on GaAs (PB-GaAs) as a platform for the detection of *Lp* was investigated in this work. PBs were grown on GaAs (001) using different "grafting-to" and "grafting-from" approaches, following slightly modified protocols. The "grafting-to" approach consists of an 11-mercaptoundecanoic acid (MUA) SAM formed on the surface of GaAs, to which poly(ethylene glycol)-diamine is further grafted (MUA-PEG protocol). The "grafting-from" approaches consist of the formation of a mercaptoundecyl bromoisobutyrate (MUBIB) initiator SAM, to which the glycidyl methacrylate (GMA) monomer is polymerized through atom transfer radical polymerization (ATRP), followed by the incorporation of either poly(ethylene)glycol (MUBIB-PEG protocol) or phenylboronic acid (MUBIB-PhB protocol). The consequences of substituting the standard procedure for the attachment of antibodies to COOH-terminated SAMs by PBs on the antibody and bacterial surface coverage were evaluated. The use of protein A for oriented immobilization of *Lp* antibodies was also investigated for conventional (SAM-GaAs) and PB-coated (PB-GaAs) surfaces. The combination of these powerful tools was evaluated to determine the optimal biosensing architecture for the detection of *Lp* with a DIP biosensor using GaAs/AlGaAs nanoheterostructures.

## 2. EXPERIMENTAL SECTION

**2.1. Materials.** Undoped, 625 ± 25 μm thick, semi-insulating, and double-sides polished GaAs (100) ± 0.5° substrates supplied by AXT Inc. (Fremont, CA, USA) were employed to investigate bacteria capture efficiencies. The $GaAs/Al_{0.35}Ga_{0.65}As$ nanoheterostructure (12 nm GaAs and 10 nm AlGaAs), grown on GaAs (100) by metal organic vapor phase epitaxy (Wafer D3422), was employed for detecting bacteria with a DIP biosensor.[20] Semiconductor-grade OptiClear, acetone, and isopropyl alcohol, used for cleaning the GaAs substrates, were purchased from National Diagnostics (Atlanta, GA, USA), ACP Chemicals (Saint-Léonard, QC, Canada), and Fisher Scientific (Ottawa, ON, Canada), respectively. Ammonium hydroxide (28%, Anachemia, Lachine, QC, Canada), anhydrous ethanol (Commercial Alcohols Inc., Brampton, ON, Canada), and methanol (VWR Chemicals, Mont-Royal, QC, Canada) were used as received.

3-aminophenylboronic acid, MUA (98%), 11-mercapto-1-undecanol (97%), α-bromoisobutyryl bromide (98%), ammonium chloride, dichloromethane (anhydrous, ≥99.8%), diethyl ether (anhydrous, ≥99.7%), 4-dimethylaminopyridine, 2-N,N′-(dimethylamino)ethyl metacrylate (98%), copper(II) bromide ($CuBr_2$, 99.999%), 2,2′-bipyridyl (>99%), *N*,*N*-dimethylformamide (DMF), ethanolamine hydrochloride, glutaric anhydride, GMA (97%), hexane (anhydrous, 95%), L-ascorbic acid, magnesium sulfate, MES buffer, poly(ethylene glycol)-diamine ($M_n$ 2000), pyridine (99.8%), toluene, and triethylamine were purchased from Sigma-Aldrich (Oakville, ON, Canada) and used without further purification.

N-hydroxysuccinimide (NHS) and N-(3-dimethylaminopropyl)-N′-ethylcarbodiimide hydrochloride (EDC) used for activation were prepared from an amine coupling kit purchased from GE Healthcare Canada (Mississauga, ON, Canada). Deoxygenated ethanol solutions (typically 40 mL) were prepared by flushing with a 3 SCFH high-purity nitrogen (99.9995%) stream (Praxair, Longueuil, QC, Canada) for 1 h. Deionized water at 18.2 MΩ $cm^{-1}$ was obtained with a Millipore purification custom system built by Culligan (Granby, QC, Canada).

Unconjugated polyclonal IgG rabbit antibodies against *Lp* and Protein A from *Staphylococcus aureus* were obtained from Virostat, Inc. (Portland, ME, USA) and Sigma-Aldrich (Oakville, ON, Canada), respectively, and then stored at −20 °C.

*Lp* ssp1, a transformed strain with an IPTG-inductive plasmid producing Green fluorescent protein (GFP) maintained by chloramphenicol was kindly provided by Prof. Sébastien Faucher (McGill University, Montréal, QC, Canada). *Lp* was first cultured on L-cysteine buffered charcoal yeast extract (VWR) and supplemented with 1 mM IPTG (Sigma Aldrich) and 5 mg/mL of chloramphenicol (Sigma


https://doi.org/10.1021/acsomega.2c03959
ACS Omega 2022, 7, 33349−33357

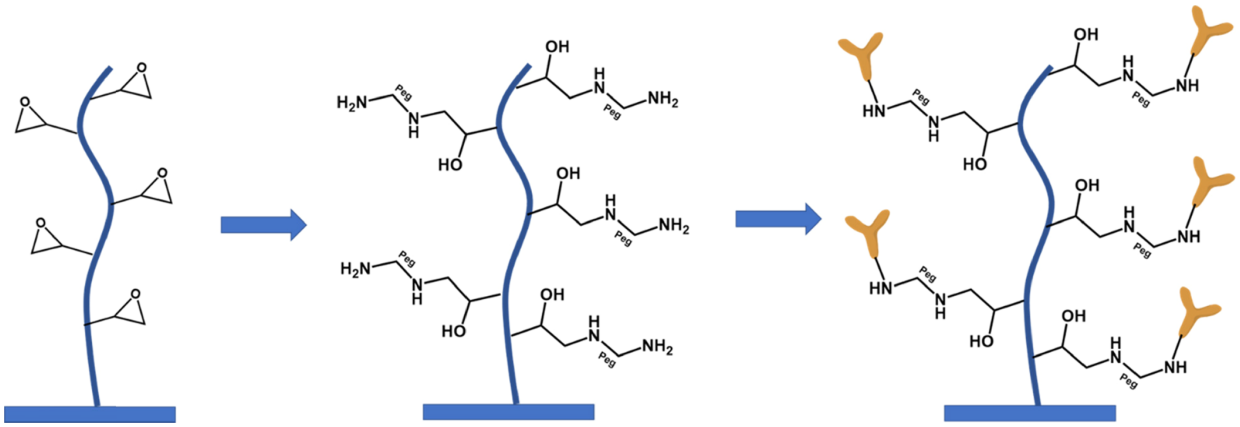

**Figure 1.** Graphical representation of a polymer brush-functionalized surface of a GaAs-based biochip.

Aldrich) at 35 °C for 4−7 days. From this culture, few colonies were suspended in 1× phosphate-buffered saline (PBS, pH 7.4) solution (Sigma Aldrich). The concentrations of *Lp* suspensions were verified by $OD_{600nm}$ measurements (0.1 $OD_{600nm}$ = 6.4 × $10^7$ CFU/ml). To inactivate *Lp*, the prepared suspensions were heat-treated at 90 °C for 20 min.

**2.2. Sample and PB Preparation.** *2.2.1. Preparation of GaAs and GaAs/AlGaAs Chips.* GaAs and GaAs/AlGaAs chips (2 mm × 2 mm) were prepared for functionalization by sequential cleaning in ultrasonic baths of acetone, OptiClear, acetone, and isopropanol for 5 min in each solvent. Then, the chips were dried under a flow of high purity (99.9995%) $N_2$ and etched in 28% ammonium hydroxide for 2 min to remove the native oxides. Finally, the chips were thoroughly rinsed with deoxygenated ethanol and immediately incubated in designated thiol solutions.

*2.2.2. Synthesis of Mercaptoundecanoic Acid-Polyethylene Glycol PBs on GaAs.* After cleaning and etching, GaAs substrates were immediately submerged in a 2 mM MUA solution prepared in deoxygenated ethanol and incubated for 20 h (4 h under agitation and 16 h in static conditions). After incubation, GaAs substrates functionalized with MUA SAMs (**MUA-GaAs**) were thoroughly rinsed with deoxygenated ethanol, followed by ultrasonic cleaning for 30 s in deoxygenated ethanol to remove the physisorbed thiols and drying under $N_2$ flow.

Following the formation of the MUA-SAM on the GaAs surface, the COOH groups of MUA were activated by incubating the substrates for 30 min in EDC (0.4 M)/NHS (0.1 M) amine coupling solution prepared in deionized water. Unreacted EDC and NHS molecules were removed by thoroughly washing the substrates with deionized water followed by their incubation overnight in a polyethylene glycol-diamine solution (50 mg/mL) prepared in MES (**A-MUA-PEG-GaAs**) or in DMF (**B-MUA-PEG-GaAs**). Finally, the obtained samples were thoroughly washed with deionized water, dried under a flow of $N_2$, and stored in sterilized individual Eppendorf tubes.

*2.2.3. Synthesis of GMA PBs on GaAs.* GMA PBs were prepared on GaAs through ATRP. The detailed protocol of the synthesis of the ATRP initiator (ω-MUBIB) and its $^1$H NMR characterization have been previously reported.[36]

The freshly etched GaAs substrates were immersed in a 2 mM solution of MUBIB prepared in deoxygenated ethanol. After 20 h of incubation (4 h under agitation and 16 h in static conditions), GaAs substrates functionalized with MUBIB SAMs (MUBIB-GaAs) were thoroughly rinsed with deoxygenated ethanol, followed by ultrasonic cleaning for 30 s in deoxygenated ethanol and drying under $N_2$ flow. Subsequently, MUBIB-GaAs substrates were immersed in a solution containing 2,2′-bipyridyl (15 mM), $CuBr_2$ (5 mM), GMA (1%, v/v), and ascorbic acid (7 mM) in methanol/water (1:1 v/v) for 5 min under agitation. Upon polymerization, MUBIB-Ep-GaAs samples were rinsed thoroughly with (1:1) methanol/water and dried under $N_2$ flow. Polyethylene glycol diamine moieties were incorporated to MUBIB-Ep-GaAs samples following part of a procedure reported by Piehler et al.[37] A solution of PEG-diamine (50 mg/mL) prepared in DMF was directly deposited on MUBIB-Ep-GaAs samples followed by incubation at 75 °C for 36 h. The obtained samples (**MUBIB-PEG-GaAs**) were then thoroughly washed with DMF and dried under $N_2$ flow.

In parallel, phenylboronic acid moieties were incorporated to MUBIB-Ep-GaAs samples following the procedure reported by Liu et al.[38] The samples were incubated in a solution containing 3-aminophenylboronic acid (50 mM) in methanol/water (1:1, v/v) for 1 h at room temperature under agitation. Following the incubation, the obtained samples (**MUBIB-PhB-GaAs**) were thoroughly washed with (1:1) methanol/water and dried under $N_2$ flow.

A detailed graphical representation of SAM formation on GaAs followed by PB attachment through different approaches has been previously reported.[36]

**2.3. Antibody Grafting on SAM-GaAs and PB-GaAs.** The antibody grafting on MUA-GaAs and MUBIB-PEG-GaAs was performed by incubation of the samples for 30 min in EDC/NHS solution for activation. Then the samples were washed with deionized water and incubated for 1 h in unconjugated IgG anti-*Lp* at a concentration of 100 μg/mL prepared in PBS 1× (pH 7.4).

For MUA-PEG-GaAs, the antibody incorporation was achieved by incubating the samples overnight in a 5 M glutaric anhydride solution prepared in DMF to transform the PEG amino groups into carboxylic acids. Then, the samples were incubated in EDC/NHS solution for 30 min, followed by incubation in anti-*Lp* antibody solution for 1 h.

The antibody immobilization on MUBIB-GaAs was ensured by incubating the samples in anti-*Lp* antibody solution for 1 h.



https://doi.org/10.1021/acsomega.2c03959
ACS Omega 2022, 7, 33349−33357

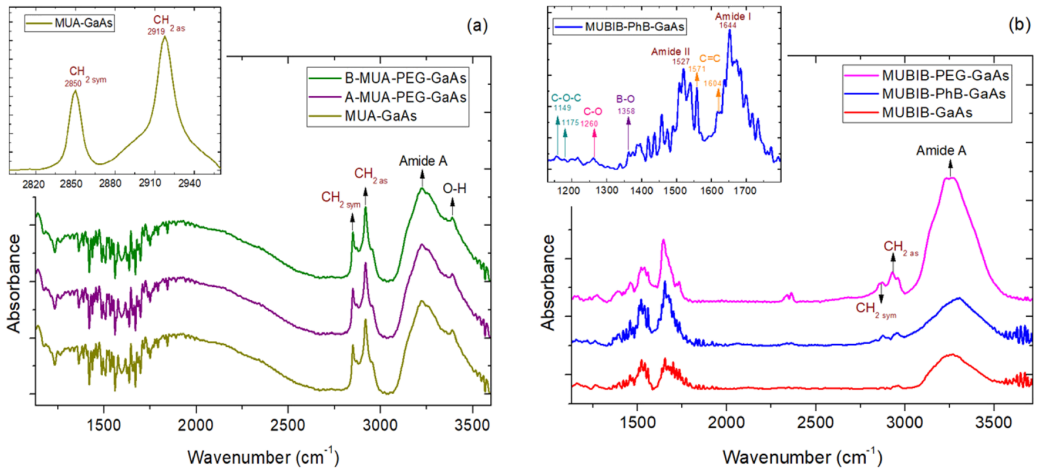


**Figure 2.** FTIR absorbance spectra of anti-*Lp* antibodies immobilized on (a) MUA SAM- and MUA-based PB-coated GaAs samples and (b) MUBIB SAM- and MUBIB-based PB- coated GaAs samples. Each spectrum represents an example of one of three tested samples.

Finally, for MUBIB-PhB PBs, the antibodies were incorporated by simple incubation in anti-*Lp* antibody solution for 1 h.

Figure 1 illustrates schematically the process of grafting the antibodies on the PB-functionalized surface of a GaAs-based biochip.

In the case of samples incorporating protein A, the antibodies were attached after the incubation of the EDC/NHS-processed samples in protein A solution prepared at 50 $\mu$g/mL in 1× PBS. All incubations were performed at room temperature and in darkness. In order to quantify the number of antibodies immobilized on the surface, Fluorescein IsoThioCyanate (FITC) antibodies against *Lp* were used for the experiments involving fluorescence measurements.

After incubation in anti-*Lp* solutions, all samples were thoroughly rinsed with 1× PBS. For the samples undergoing FTIR or fluorescence measurements, the rinsing was done with deionized water followed by drying under $N_2$ flow.

**2.4. Bacteria Capture Experiments.** To minimize nonspecific interactions, a blocking step of the surface was conducted by incubating the samples in ethanolamine (1 M, pH 8) for 30 min, followed by rinsing with 1× PBS. Because of its small size, ethanolamine fills the interstices where the antibody or protein A could not be grafted due to their bulkiness. After blocking, the antibody-functionalized samples were incubated for 1 h in a $10^5$ CFU/mL suspension of inactivated *Lp*, prepared in 1× PBS following the dilution of a freshly prepared culture. Upon incubation, the samples were rinsed with 1× PBS, followed by rinsing with deionized water and drying under $N_2$ flow.

**2.5. DIP Experiments.** The MUBIB/antibody-functionalized GaAs/AlGaAs chips were installed in a polyetherimide holder equipped with a quartz window allowing to carry out irradiation with a homogenized beam of a 375 nm light emitting diode delivering 50 mW/cm$^2$ power to the chip surface. The intermittent irradiation with a duty cycle of 1.5 s in each 11 s allowed for recording the PL signal and determining DIP rates based on time-dependent location of PL intensity maxima using a custom-designed quantum semiconductor photonic biosensing reader (QSPB-3).

Different suspensions of bacteria were run through the flow cell at 40 $\mu$L/min for 25 min, and then additional 5 min were allowed to capture bacteria on the biochip surface. This was followed by flowing 0.1× PBS solution for 10 min designed to wash loosely bonded bacteria.

The DIP experiments were carried out in a 0.1× PBS solution, and the runs without bacteria were used to obtain the reference signal. All DIP experiments were repeated at least three times for each bacterial concentration.

**2.6. FTIR and Fluorescence Microscopy Diagnostics.** FTIR transmission spectra were recorded to evaluate the binding of thiols and PBs to the GaAs surface, as well as the efficiency of antibody grafting for different architectures. The measurements were performed under vacuum using a Bruker Vertex 70v spectrometer, equipped with a RockSolid interferometer and a wide-range Globar IR source covering 6000 to 10 cm$^{-1}$. The spectra (1000 scans) were collected with a liquid-nitrogen-cooled mercury cadmium telluride IR detector at 4 cm$^{-1}$ spectral resolution and an aperture of 1.5 mm. The spectrum of a freshly etched GaAs substrate was used as reference and subtracted from the spectra of biofunctionalized samples.

The presence of fluorescence labeled antibodies or bacteria immobilized on the surface of the biochips was analyzed using an Olympus IX71 fluorescence microscope equipped with GFP filters (excitation at 473 nm and emission at 520 nm), FITC (excitation at 495 nm, emission at 519 nm), and a DP71 digital camera. Six to eight images were collected per sample at different sites with a 20× magnification using Q-capture software (QImaging Corporation, Surrey, BC, Canada). The number of antibodies/bacteria present on the surface was estimated for each sample after analysis of the fluorescent images with ImageJ software.[39]

## 3. RESULTS AND DISCUSSION

**3.1. Assessment of the Antibody Grafting Efficiency on SAM-GaAs and PB-GaAs Surfaces.** Efficient immobilization of antibodies to the SAM- or PB-functionalized surface is crucial for the immunological recognition activity and, consequently, the operation of the biosensor. Antibody immobilization in random orientation on a solid substrate may result in unexpected denaturation and shielding of their active binding sites. Thus, partial or complete loss of its bioactivity may occur due to steric hindrance and change of active site conformation during the immobilization.[25] Con-


https://doi.org/10.1021/acsomega.2c03959
ACS Omega 2022, 7, 33349−33357

sequently, qualitative and quantitative characterization of the antibody-functionalized samples, with and without protein A, was performed using FTIR and fluorescence microscopy.

*3.1.1. FTIR Analysis of Thiol, PBs, and Antibody Binding.* FTIR characteristic peaks were analyzed for confirmation of the successful formation of SAMs and PBs through the presence of the functional groups needed for further antibody attachment. The spectra of compounds used for the synthesis of SAM-GaAs and PB-GaAs samples have been previously reported.[36] Figure 2 shows the FTIR absorbance spectra obtained for SAM-GaAs and PB-GaAs samples upon incubation for 1 h in IgG anti-*Lp* antibodies. As it can be seen, the absorption bands at 1149, 1175, and 1260 $cm^{-1}$ correspond to C−O−C and C−O stretching, respectively. These three characteristic bands of epoxy groups are clearly observed from GMA, demonstrating its successful grafting. The band at 1358 $cm^{-1}$ has been previously assigned to B−O stretching, while the bands at 1604 and 1571 $cm^{-1}$ correspond to the C═C stretching of the benzene ring.[38] These results confirm the successful conjugation of phenylboronic acid to MUBIB-Ep.

The bands observed at 2919 and 2850 $cm^{-1}$ are typical of the $-CH_2$ asymmetric and symmetric vibrations, respectively, and are assigned to the thiol groups, complying with the reported literature.[40] The FTIR characteristics of these vibrations suggest the formation of high quality SAMs of MUA and MUBIB.

The presence of antibodies covalently immobilized on the surface was studied by FTIR probing of the amide bands A, I, and II located in the regions of 3296, 1644, and 1527 $cm^{-1}$ and associated with the N−H, C═O, and C−N stretching vibrations, respectively. The amide A peak is the most intense and least noisy among the amide bands. The antibody immobilization efficiency was evaluated by calculating its integrated absorbance intensity (the area under the amide A peak) that was proportional to the concentration of antibodies. Consequently, the values of the amide A-integrated absorbance intensity (in the range of 3050 to 3550 $cm^{-1}$) were determined for each architecture by using a Lorentz fitting and reported in Table 1.

**Table 1. Amide A Peak Values of Anti-*Lp* Antibodies Measured by FTIR for SAM-GaAs and PB-GaAs Samples**

| architecture | absorbance ± $\sigma^a$ | integrated absorbance intensity ± $\sigma^a$ |
|---|---|---|
| MUA-GaAs | $9.93 \times 10^{-4} \pm 9.55 \times 10^{-5}$ | 0.28 ± 0.02 |
| A-MUA-PEG-GaAs | $1.24 \times 10^{-3} \pm 1.06 \times 10^{-4}$ | 0.36 ± 0.04 |
| B-MUA-PEG-GaAs | $1.57 \times 10^{-3} \pm 1.24 \times 10^{-4}$ | 0.57 ± 0.06 |
| MUBIB-GaAs | $1.25 \times 10^{-3} \pm 1.08 \times 10^{-4}$ | 0.42 ± 0.02 |
| MUBIB-PhB-GaAs | $1.60 \times 10^{-3} \pm 1.37 \times 10^{-4}$ | 0.82 ± 0.04 |
| MUBIB-PEG-GaAs | $4.56 \times 10^{-3} \pm 3.59 \times 10^{-4}$ | 1.65 ± 0.11 |

[a]Standard deviation determined from three experimental replicates.

It can be seen that the integrated absorbance of the amide A feature over the range 3050−3550 $cm^{-1}$ is significantly greater for MUBIB-based SAMs and PBs, indicating the immobilization of a higher number of antibodies as compared to MUA-based SAMs and PBs. Furthermore, higher absorbance and integrated intensity values were determined for PBs as compared to the conventional SAM architecture, suggesting that PBs allow the immobilization of a higher number of antibodies through their three-dimensional structure.

*3.1.2. Evaluation of the Antibody-Surface Coverage.* The estimation of the number of antibody clusters grafted per $mm^2$ was obtained for each architecture from the fluorescence microscopy images. The comparison of fluorescence images of B-MUA-PEG PBs taken before and after the attachment of fluorescent-labeled antibodies, is presented in Figure 3. The absence of fluorescence before antibody attachment in contrast with the fluorescence observed after treating the SAM and PBs samples with FITC-antibodies confirms the compatibility of the former with such target recognition agents. Similar results were obtained for the other studied approaches.

It can also be seen that the antibody surface coverage was significantly increased when protein A was incorporated in the immobilization protocol, achieving well-ordered IgG-binding proteins, which further enhanced the oriented grafting of antibodies.

Figure 4 summarizes the antibody surface coverage results for each approach considered in this study, obtained upon incubation of SAM-GaAs and PB-GaAs samples in IgG anti-*Lp* suspensions. As expected, the antibody surface coverage values achieved for PBs were significantly higher in comparison with the conventional SAMs, confirming the compatibility of the PB-GaAs platform with anti-*Lp* and validating the superior performance of this 3D architecture. A higher antibody surface coverage (∼4 times) was obtained for B-MUA-PEG as compared to A-MUA-PEG PBs, suggesting that dissolving PEG in DMF rather than MES buffer improved diamino-PEG solubility at the time of its incorporation, which has been previously demonstrated by the PB roughness factor.[36] A significant improvement of the number of immobilized antibodies was recorded with the use of protein A (∼1.5 to 2 times for A-MUA-PEG and B-MUA-PEG PBs, respectively, and up to 5 times in the case of MUA SAM), resulting in homogenous attachment of antibodies in a preferable orientation, which prevents undesired conformational changes and the insufficient exposure of functional domains.

Representative micrographs of FITC anti-*Lp* immobilized on MUBIB SAMs and PBs, with and without protein A, are shown in Figure S1. In the case of MUBIB SAMs, an increase of only 25% in antibody surface coverage was observed when protein A was added. On the other hand, the incorporation of protein A for the immobilization of antibodies on MUBIB-PhB and MUBIB-PEG PBs allowed us to attach antibodies with 2.5 to 3 times higher efficiency, respectively, which is consistent with the role of this molecule in enhancing the antibody immobilization event.

The uneven antibody distribution obtained for MUBIB-based PBs, giving rise to the high standard deviations shown in Figure 4b, is likely due to the relatively irregular distribution of PBs. It is relevant to note that MUBIB-PEG PBs gave rise to considerably higher and more uniform antibody surface coverage, suggesting that the PEG termination provides better compatibility with the amine group of antibodies. Based on these results, it would be possible to monitor the sensitivity of the biosensor by tuning the PB-GaAs interface through modification of the end functional group, which would affect its spatial disposition and availability to interact with the corresponding antibodies.

**3.2. Immobilization of *Lp* Using SAM-GaAs and PB-GaAs.** The number of bacteria captured per $mm^2$ for each



https://doi.org/10.1021/acsomega.2c03959
ACS Omega 2022, 7, 33349−33357

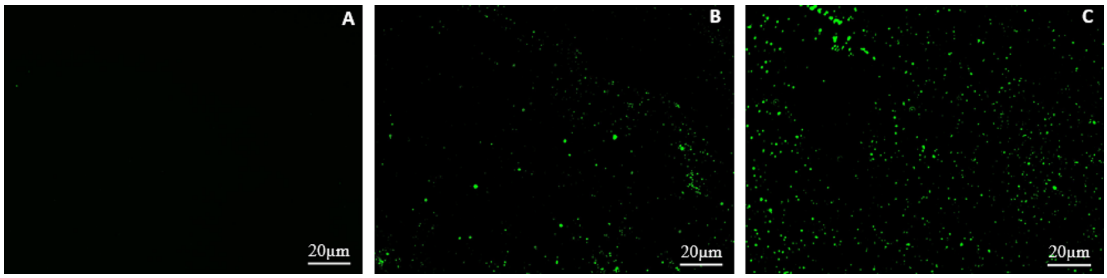


**Figure 3.** Fluorescence microscopy images of B-MUA-PEG before their incubation in anti-*Lp* suspension (A) and after the grafting of FITC-labeled antibodies in the absence (B) and presence (C) of protein A.

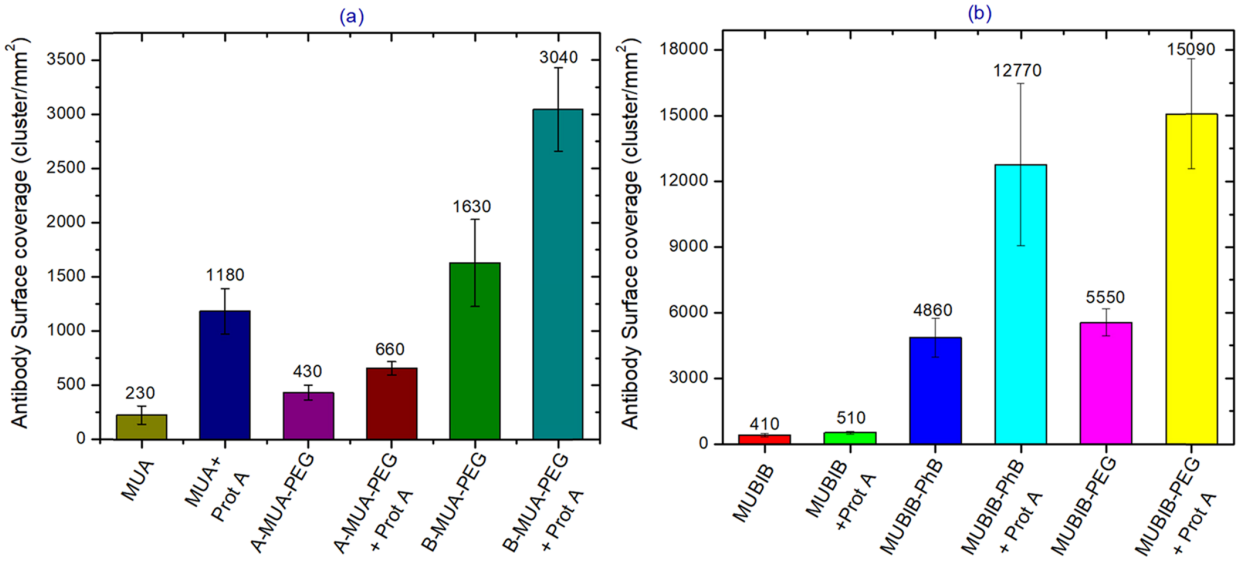


**Figure 4.** Surface coverage of FITC antibodies against *Lp* immobilized with and without protein A on (a) MUA SAM- and MUA-based PB-coated GaAs samples; (b) MUBIB SAM- and MUBIB-based PB-coated GaAs samples.

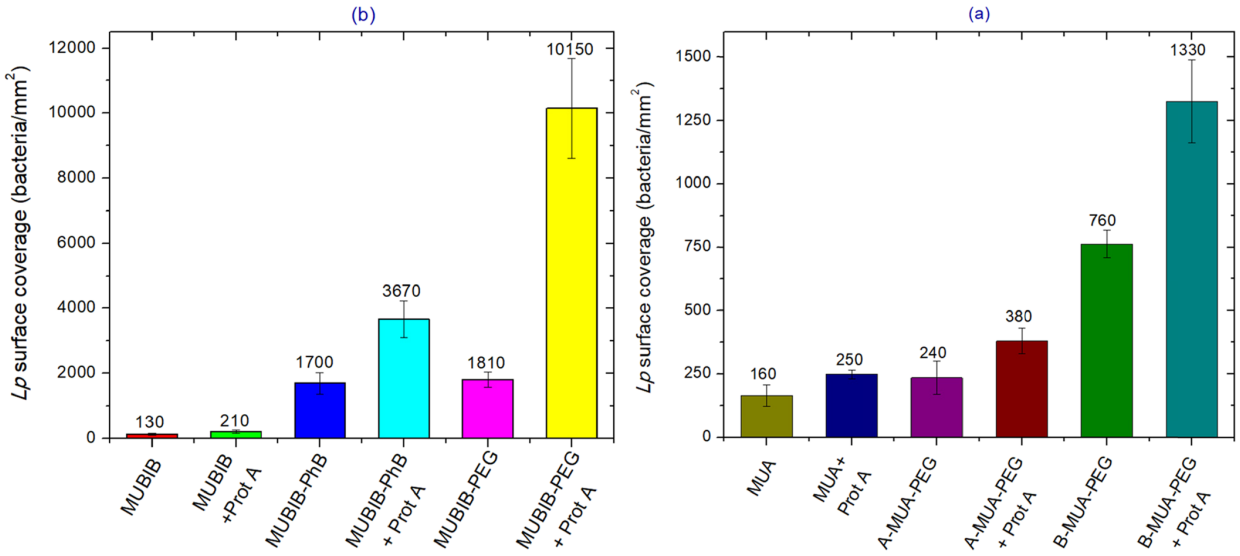


**Figure 5.** Surface coverage of captured GFP *Lp* on the surface of (a) MUA SAM- and MUA-based PB-coated GaAs samples and (b) MUBIB SAM- and MUBIB-based PB-coated GaAs samples, with and without protein A.



https://doi.org/10.1021/acsomega.2c03959
*ACS Omega* 2022, 7, 33349−33357

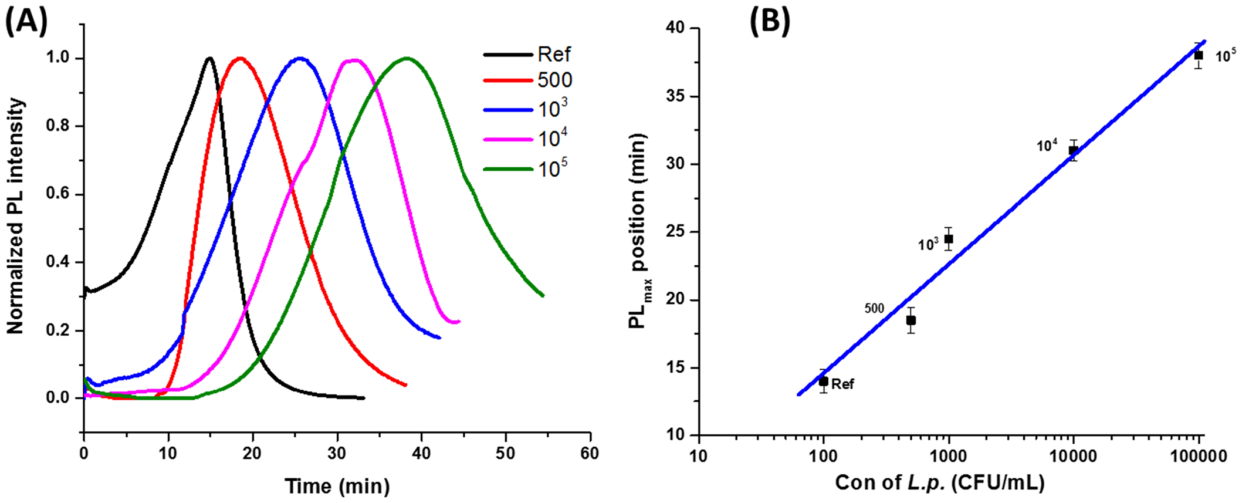


**Figure 6.** Representative temporal PL intensity plots of GaAs/AlGaAs polymer brush (MUBIB-PEG)-functionalized biochips digitally photocorroding (Duty Cycle = 1.5/11) under continuous flow of 0.1× PBS and different concentrations of bacteria (A). Calibration curve based on the position of the PL intensity maximum revealed with the digital photocorrosion process for the GaAs (12 nm)/AlGaAs (10 nm) nanoheterostructure (B).

sensing architecture was obtained from the fluorescence images, as summarized in Figure 5. The average bacteria coverage values determined for MUBIB-PhB-GaAs (1697 ± 326 bacteria/mm$^2$) and MUBIB-PEG-GaAs (1852 ± 237 bacteria/mm$^2$) were found to be comparable, in the limit of the error, at the tested incubation concentration of $10^5$ CFU/mL. These values were almost 2 times higher than the bacterial surface coverage obtained for B-MUA-PEG PBs (763 ± 55 bacteria/mm$^2$) and up to 10 times higher than that obtained for the conventional thiol-based architectures tested in this work (129 ± 37 bacteria/mm$^2$ for MUBIB SAMs and 164 ± 42 bacteria/mm$^2$ for MUA SAMs) and to what has been previously reported for optimized non-PB-based GaAs biosensors coupled with sensitive detection techniques.[15,16,19,20] A coverage increase of 2 times was observed when protein A was added to B-MUA-PEG-GaAs and MUBIB-PhB-GaAs samples, while MUBIB-PEG-GaAs recorded a 5.5 times higher surface coverage when protein A was incorporated in the antibody immobilization process, demonstrating the positive impact of protein A functionalization in increasing the efficiency of *Lp* recognition.

Figure S2 shows representative fluorescence images of *Lp* captured using each approach. The uneven bacterial distribution, giving rise to relatively high standard deviations, was likely due to less uniform distribution of PBs. Nevertheless, the number of attached bacteria was sufficient to confirm the feasibility of using the PB-GaAs platform for bacteria capture and its advantage compared to the conventional SAM architecture.

Out of the approaches considered in this study, MUBIB-PEG seems to be the most promising architecture since it provided higher surface coverage and lower variability in antibody and bacteria surface coverage compared to the other PB architectures studied in this work.

**3.3. Detection of *Lp* with a DIP Biosensor.** A series of PL intensity plots collected with DIP biochips functionalized with the MUBIB-PEG PB-architecture and exposed in 0.1× PBS to *Lp* suspensions at 500, $10^3$, $10^4$, and $10^5$ CFU/mL is shown in Figure 6A. The formation of PL intensity maximum ($PL_{max}$) observed in each case is a characteristic of the DIP process related to the photocorrosion front crossing the interface between GaAs (12 nm thick) and $Al_{0.35}Ga_{0.65}As$ (10 nm thick) layers. The interaction between negatively charged bacteria and the biochip surface results in reduced photocorrosion rates and, consequently, the positions of $PL_{max}$ are delayed proportionally to the surface captured bacteria.[15,16] This effect is related to the electron transfer from bacteria and reduced band bending of the semiconductor biochip. Of particular interest is that the $PL_{max}$ recorded for 500 CFU/mL appears ∼4.5 min delayed in comparison to the $PL_{max}$ (Ref) observed at 14 min. This result, compared to the limit of detection of *Lp* at $10^3$−$10^4$ CFU/mL commonly reported with traditional biosensors, proves attractiveness of the proposed PB-based biosensing architecture. The calibration curve shown in Figure 6B also illustrates the attractive range of a linear response on the semi-logarithmic scale of the constructed DIP biosensor ranging between 500 and $10^5$ CFU/mL.

## 4. CONCLUSIONS

We have explored the innovative concept of biofunctionalization of GaAs/AlGaAs nanoheterostructures with PBs as a platform for enhanced detection of *Legionella pneumophila* with a DIP biosensor. The attractive three-dimensional character of a MUBIB-polyethylene glycol (PEG) architecture employed for the capture of antibodies allowed to immobilize the eightfold greater concentration of *L. pneumophila* than that achieved with the standard biofunctionalization of GaAs employing antibodies linked with MUA COOH-terminated SAMs. The enhanced efficiency in capturing bacteria has been verified with a DIP GaAs/AlGaAs biosensor reporting the attractive limit of detection of *L. pneumophila* at 500 CFU/mL. This represents a significant improvement in achieving an attractive limit of detection compared to those reported with conventional biosensors. Furthermore, the incorporation of antibodies through tunable functional groups of MUBIB architectures suggests the possibility of employing different biosensing devices targeting also other bacteria and biomolecules.


https://doi.org/10.1021/acsomega.2c03959
ACS Omega 2022, 7, 33349−33357

## ■ ASSOCIATED CONTENT

### Supporting Information

The Supporting Information is available free of charge at https://pubs.acs.org/doi/10.1021/acsomega.2c03959.

Representative fluorescence micrographs of FITC-labeled anti-*Lp* on MUBIB-GaAs, MUBIB-PhB-GaAs, and MUBIB-PEG-GaAs samples, with and without protein A, and representative fluorescence micrographs of GFP *Lp* immobilized on MUBIB-GaAs, MUBIB-PhB-GaAs, and MUBIB-PEG-GaAs samples, with and without protein A (PDF)

## ■ AUTHOR INFORMATION


### Corresponding Author

**Jan J. Dubowski** − *Interdisciplinary Institute for Technological Innovation (3IT), CNRS UMI-3463, Université de Sherbrooke, Sherbrooke, Québec J1K 0A5, Canada;* orcid.org/0000-0003-0022-527X; Email: Jan.J.Dubowski@USherbrooke.ca

### Authors

**Juliana Chawich** − *Interdisciplinary Institute for Technological Innovation (3IT), CNRS UMI-3463, Université de Sherbrooke, Sherbrooke, Québec J1K 0A5, Canada*

**Walid M. Hassen** − *Interdisciplinary Institute for Technological Innovation (3IT), CNRS UMI-3463, Université de Sherbrooke, Sherbrooke, Québec J1K 0A5, Canada*

**Amanpreet Singh** − *Interdisciplinary Institute for Technological Innovation (3IT), CNRS UMI-3463, Université de Sherbrooke, Sherbrooke, Québec J1K 0A5, Canada*

**Daniela T. Marquez** − *Interdisciplinary Institute for Technological Innovation (3IT), CNRS UMI-3463, Université de Sherbrooke, Sherbrooke, Québec J1K 0A5, Canada; Department of Chemistry, Carleton University, Ottawa, Ontario K1S 5B6, Canada*

**Maria C. DeRosa** − *Department of Chemistry, Carleton University, Ottawa, Ontario K1S 5B6, Canada*

Complete contact information is available at: https://pubs.acs.org/10.1021/acsomega.2c03959


### Notes

The authors declare no competing financial interest.

## ■ ACKNOWLEDGMENTS

This project was supported by the Natural Sciences and Engineering Research Council of Canada Strategic Partnership Grant No. SPG-2016-494057 and by the NSERC Discovery Grant RGPIN 2015-04448. The authors declare no conflict of interest.

## ■ REFERENCES


(1) Berjeaud, J.-M.; Chevalier, S.; Schlusselhuber, M.; Portier, E.; Loiseau, C.; Aucher, W.; Lesouhaitier, O.; Verdon, J. *Legionella pneumophila*: The paradox of a highly sensitive opportunistic waterborne pathogen able to persist in the environment. *Front. Microbiol.* **2016**, *7*, 486.

(2) Hamilton, K. A.; Prussin, A. J.; Ahmed, W.; Haas, C. N. Outbreaks of Legionnaires' disease and Pontiac fever 2006−2017. *Curr. Environ. Health Rep.* **2018**, *5*, 263−271.

(3) Gonçalves, I. G.; Fernandes, H. S.; Melo, A.; Sousa, S. F.; Simões, L. C.; Simões, M. *LegionellaDB* - A database on *Legionella* outbreaks. *Trends Microbiol.* **2021**, *29*, 863−866.

(4) Wüthrich, D.; Gautsch, S.; Spieler-Denz, R.; Dubuis, O.; Gaia, V.; Moran-Gilad, J.; Hinic, V.; Seth-Smith, H. M.; Nickel, C. H.; Tschudin-Sutter, S.; Bassetti, S.; Haenggi, M.; Brodmann, P.; Fuchs, S.; Egli, A. Air-conditioner cooling towers as complex reservoirs and continuous source of *Legionella pneumophila* infection evidenced by a genomic analysis study in 2017, Switzerland. *Euro Surveill.* **2019**, *24*, No. 1800192.

(5) Lévesque, S.; Plante, P. L.; Mendis, N.; Cantin, P.; Marchand, G.; Charest, H.; Raymond, F.; Huot, C.; Goupil-Sormany, I.; Desbiens, F.; Faucher, S. P.; Corbeil, J.; Tremblay, C. Genomic characterization of a large outbreak of *Legionella pneumophila* serogroup 1 strains in Quebec City, 2012. *PLoS One* **2014**, *9*, No. e103852.

(6) Herwaldt, L. A.; Marra, A. R. *Legionella*: a reemerging pathogen. *Curr. Opin. Infect. Dis.* **2018**, *31*, 325−333.

(7) De Lorenzis, E.; Manera, M. G.; Montagna, G.; Cimaglia, F.; Chiesa, M.; Poltronieri, P.; Santino, A.; Rella, R. SPR based immunosensor for detection of *Legionella pneumophila* in water samples. *Opt. Commun.* **2013**, *294*, 420−426.

(8) Dusserre, E.; Ginevra, C.; Hallier-Soulier, S.; Vandenesch, F.; Festoc, G.; Etienne, J.; Jarraud, S.; Molmeret, M. A PCR-based method for monitoring *Legionella pneumophila* in water samples detects viable but noncultivable *Legionellae* that can recover their cultivability. *Appl. Environ. Microbiol.* **2008**, *74*, 4817−4824.

(9) Boss, R.; Baumgartner, A.; Kroos, S.; Blattner, M.; Fretz, R.; Moor, D. Rapid detection of viable *Legionella pneumophila* in tap water by a qPCR and RT-PCR-based method. *J. Appl. Microbiol.* **2018**, *125*, 1216−1225.

(10) Dilger, T.; Melzl, H.; Gessner, A. Rapid and reliable identification of waterborne *Legionella* species by MALDI-TOF mass spectrometry. *J. Microbiol. Methods* **2016**, *127*, 154−159.

(11) Mobed, A.; Hasanzadeh, M.; Agazadeh, M.; Mokhtarzadeh, A.; Rezaee, M. A.; Sadeghi, J. Bioassays: The best alternative for conventional methods in detection of *Legionella pneumophila*. *Int. J. Biol. Macromol.* **2019**, *121*, 1295−1307.

(12) Meneghello, A.; Sonato, A.; Ruffato, G.; Zacco, G.; Romanato, F. A novel high sensitive surface plasmon resonance *Legionella pneumophila* sensing platform. *Sens. Actuators B Chem.* **2017**, *250*, 351−355.

(13) Li, N.; Brahmendra, A.; Veloso, A. J.; Prashar, A.; Cheng, X. R.; Hung, V. W. S.; Guyard, C.; Terebiznik, M.; Kerman, K. Disposable immunochips for the detection of *Legionella pneumophila* using electrochemical impedance spectroscopy. *Anal. Chem.* **2012**, *84*, 3485−3488.

(14) Chawich, J.; Hassen, W. M.; Elie-Caille, C.; Leblois, T.; Dubowski, J. J. Regenerable ZnO/GaAs bulk acoustic wave biosensor for detection of *Escherichia coli* in 'complex' biological medium. *Biosensors* **2021**, *11*, 145.

(15) Aziziyan, M. R.; Hassen, W. M.; Morris, D.; Frost, E. H.; Dubowski, J. J. Photonic biosensor based on photocorrosion of GaAs/AlGaAs quantum heterostructures for detection of *Legionella pneumophila*. *Biointerphases* **2016**, *11*, 19301.

(16) Aziziyan, M. R.; Hassen, W. M.; Sharma, H.; Shirzaei Sani, E.; Annabi, N.; Frost, E. H.; Dubowski, J. J. Sodium dodecyl sulfate decorated *Legionella pneumophila* for enhanced detection with a GaAs/AlGaAs nanoheterostructure biosensor. *Sens. Actuators B Chem.* **2020**, *304*, No. 127007.

(17) Nazemi, E.; Hassen, W. M.; Frost, E. H.; Dubowski, J. J. Monitoring growth and antibiotic susceptibility of *Escherichia coli* with photoluminescence of GaAs/AlGaAs quantum well microstructures. *Biosens. Bioelectron.* **2017**, *93*, 234−240.

(18) Nazemi, E.; Aithal, S.; Hassen, W. M.; Frost, E. H.; Dubowski, J. J. GaAs/AlGaAs heterostructure based photonic biosensor for rapid detection of *Escherichia coli* in phosphate buffered saline solution. *Sens. Actuators B Chem.* **2015**, *207*, 556−562.

(19) Islam, M. A.; Hassen, W. M.; Tayabali, A. F.; Dubowski, J. J. Short ligand, Cysteine-modified warnericin RK antimicrobial peptides favor highly sensitive detection of *Legionella pneumophila*. *ACS Omega* **2021**, *6*, 1299−1308.
(20) Islam, M. A.; Hassen, W. M.; Tayabali, A. F.; Dubowski, J. J. Antimicrobial warnericin RK peptide functionalized GaAs/AlGaAs biosensor for highly sensitive and selective detection of *Legionella pneumophila*. *Biochem. Eng. J.* **2020**, *154*, No. 107435.
(21) Saad, M.; Chinerman, D.; Tabrizian, M.; Faucher, S. P. Identification of two aptamers binding to *Legionella pneumophila* with high affinity and specificity. *Sci. Rep.* **2020**, *10*, 9145.
(22) Mobed, A.; Hasanzadeh, M.; Hassanpour, S.; Saadati, A.; Agazadeh, M.; Mokhtarzadeh, A. An innovative nucleic acid based biosensor toward detection of *Legionella pneumophila* using DNA immobilization and hybridization: A novel genosensor. *Microchem. J.* **2019**, *148*, 708−716.
(23) Sharma, S.; Byrne, H.; O'Kennedy, R. J. Antibodies and antibody-derived analytical biosensors. *Essays Biochem.* **2016**, *60*, 9−18.
(24) Lebec, V.; Boujday, S.; Poleunis, C.; Pradier, C.-M.; Delcorte, A. Time-of-Flight secondary ion mass spectrometry investigation of the orientation of adsorbed antibodies on SAMs correlated to biorecognition tests. *J. Phys. Chem. C* **2014**, *118*, 2085−2092.
(25) Liu, Y.; Yu, J. Oriented immobilization of proteins on solid supports for use in biosensors and biochips: a review. *Microchim. Acta* **2016**, *183*, 1−19.
(26) Welch, N. G.; Scoble, J. A.; Muir, B. W.; Pigram, P. J. Orientation and characterization of immobilized antibodies for improved immunoassays (Review). *Biointerphases* **2017**, *12*, 02D301.
(27) Chen, W.-L.; Cordero, R.; Tran, H.; Ober, C. K. 50th Anniversary Perspective: Polymer Brushes: Novel surfaces for future materials. *Macromolecules* **2017**, *50*, 4089−4113.
(28) Kim, M.; Schmitt, K. S.; Choi, W. J.; Krutty, D. J.; Gopalan, P. From self-assembled monolayers to coatings: Advances in the synthesis and nanobio applications of polymer brushes. *Polymer* **2015**, *7*, 1346−1378.
(29) Krishnamoorthy, M.; Hakobyan, S.; Ramstedt, M.; Gautrot, J. E. Surface-initiated polymer brushes in the biomedical field: Applications in membrane science, biosensing, cell culture, regenerative medicine and antibacterial coatings. *Chem. Rev.* **2014**, *114*, 10976−11026.
(30) Kaholek, M.; Lee, W.-K.; LaMattina, B.; Caster, K. C.; Zauscher, S. Fabrication of stimulus-responsive nanopatterned polymer brushes by scanning-probe lithography. *Nano Lett.* **2004**, *4*, 373−376.
(31) Seifert, M.; Koch, A.; Deubel, F.; Simmet, T.; Hess, L. H.; Stutzmann, M.; Jordan, R.; Garrido, J.; Sharp, I. Functional polymer brushes on hydrogenated graphene. *Chem. Mater.* **2013**, *25*, 466−470.
(32) Steenackers, M.; Sharp, I. D.; Larsson, K.; Hutter, N. A.; Stutzmann, M.; Jordan, R. Structured polymer brushes on silicon carbide. *Chem. Mater.* **2010**, *22*, 272−278.
(33) Ye, Y.; Chen, L.; Krull, U. J. Light induced surface corrosion of Gallium Arsenide for immobilization of Oligonucleotide probes. *Anal. Lett.* **2008**, *41*, 289−301.
(34) Dubowski, J. J.; Voznyy, O.; Marshall, G. M. Molecular self-assembly and passivation of GaAs (001) with alkanethiol monolayers: A view towards bio-functionalization. *Appl. Surf. Sci.* **2010**, *256*, 5714−5721.
(35) Tang, L.; Chun, I. S.; Wang, Z.; Li, J.; Li, X.; Lu, Y. DNA detection using plasmonic enhanced near-infrared photoluminescence of gallium arsenide. *Anal. Chem.* **2013**, *85*, 9522−9527.
(36) Marquez, D. T.; Chawich, J.; Hassen, W. M.; Moumanis, K.; DeRosa, M. C.; Dubowski, J. J. Polymer brush−GaAs interface and its use as an antibody-compatible platform for biosensing. *ACS Omega* **2021**, *6*, 7286−7295.
(37) Piehler, J.; Brecht, A.; Valiokas, R.; Liedberg, B.; Gauglitz, G. A high-density poly(ethylene glycol) polymer brush for immobilization on glass-type surfaces. *Biosens. Bioelectron.* **2000**, *15*, 473−481.
(38) Liu, Y.; Zhang, Y.; Zhao, Y.; Yu, J. Phenylboronic acid polymer brush-enabled oriented and high density antibody immobilization for sensitive microarray immunoassay. *Colloids Surf., B: Biointerfaces* **2014**, *121*, 21−26.
(39) Schneider, C. A.; Rasband, W. S.; Eliceiri, K. W. NIH Image to ImageJ: 25 years of image analysis. *Nat. Methods* **2012**, *9*, 671−675.
(40) Lacour, V.; Moumanis, K.; Hassen, W. M.; Elie-Caille, C.; Leblois, T.; Dubowski, J. J. Formation kinetics of mixed self-assembled monolayers of alkanethiols on GaAs(100). *Langmuir* **2019**, *35*, 4415−4427.


https://doi.org/10.1021/acsomega.2c03959
*ACS Omega* 2022, 7, 33349−33357